Frozen Ground Containment Barrier

GEO-SLOPE International Ltd. | www.geo-slope.com

1200, 700 - 6th Ave SW, Calgary, AB, Canada T2P 0T8
Main: +1 403 269 2002 | Fax: +1 888 463 2239

Introduction

Frozen soil barriers can be used to isolate contaminated water within a groundwater flow system. The barrier forms because the ice within the pore space decreases the hydraulic conductivity, which in-turn causes water to divert around the frozen zone. Heat conduction occurs through the frozen and unfrozen zones. Heat advection (forced convection) with the flowing water supplements, and dominates, the heat transport in the unfrozen zone. The frozen wall example illustrates the influence of groundwater flow on the propagation of a freezing front from a frozen soil barrier.

Background

McKenzie et al. (2007) developed a hypothetical scenario that is meant to represent a frozen wall boundary typically used in groundwater contamination remediation (Figure 1). The simulation is of warm groundwater flow across a domain that comprises a partially intruding frozen wall. The frozen zone propagates both upstream and downstream, leading to an essentially impermeable zone around the original wall.

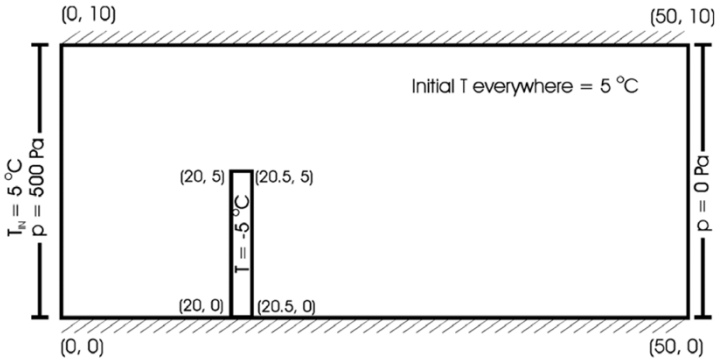

Figure 1. Problem configuration developed by McKenzie et al. (2007).

Numerical Simulation

The model domain has a height and length of 10 m and 50 m, respectively (Figure 2). The wall is 0.5 m wide and 5 m high and is located between the x-coordinate of 20 m and 20.5 m. A temperature boundary condition of -5°C is applied to the region comprising the wall for the duration of the analysis. The left edge of the domain represents the upstream boundary where warm groundwater is entering at a constant temperature of 5°C. Constant head boundary conditions of 10.05 m and 10.00 m were applied to the left and right edges of the domain, respectively. Adiabatic conditions are assumed for the top, bottom, and right boundaries of the domain.

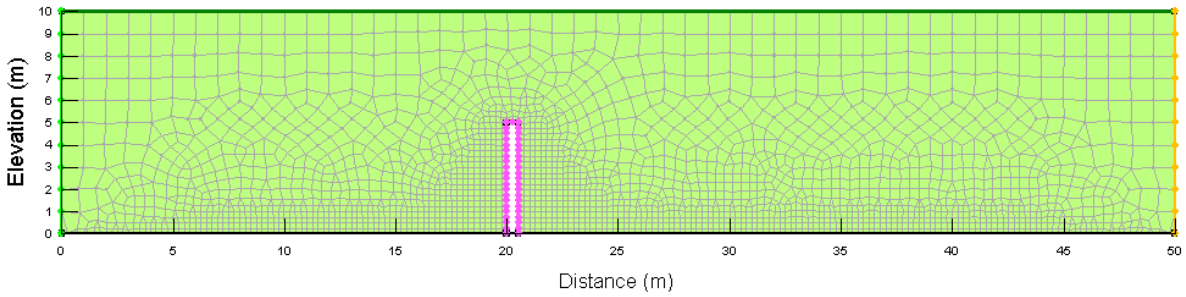

Figure 2. Problem configuration in GeoStudio.

An 800 day transient heat and water transfer simulation was completed on the same domain using an exponential time sequence with an initial increment of 1800 seconds. The heat transfer analysis simulates conduction energy transfer. Toggling on the physics option for forced convection with water transfer introduces an additional energy transfer mechanism: heat advection with flowing water (Figure 3). The transient analysis required both an initial temperature and pore-water pressure distribution. The initial pore-water pressure distribution was developed using a steady-state water transfer analysis, while the initial temperatures were established using the Activation Temperature option in the material model definition.

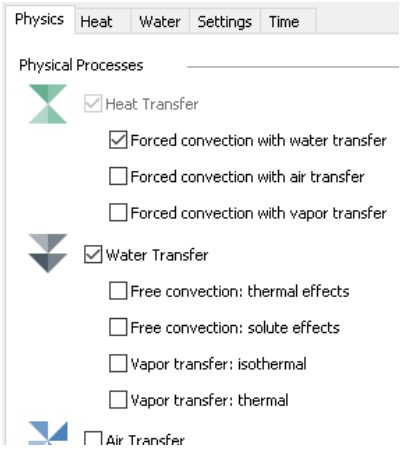

Figure 3. Physics tab for the forced-convection analysis.

The objective of this analysis is to illustrate the influence of pore-ice blockage on groundwater flow, not to replicate the simulated response shown by McKenzie et al. (2007). As such, the hydraulic and

thermal properties used in the analysis were based on those presented by McKenzie et al. (2007), but not replicated exactly (Table 1).

Table 1. Input variables for the calculated thermal material properties.

Thermal Property	Input variable
Specific Heat of Fluid	4182 J/kg/°C
Specific Heat of Ice	2108 J/kg/°C
Specific Heat of Solids	840 J/kg/°C
Thermal Conductivity of Fluid	0.6 J/sec/m/°C
Thermal Conductivity of Ice	2.14 J/sec/m/°C
Thermal Conductivity of Solids	3.5 J/sec/m/°C
Soil density	2600 kg/m^3
Ice density	920 J/kg
Water density	1000 kg/m^3
Porosity	0.1
S_{wres}	0.05

The water transfer formulation does not normally acknowledge the presence of ice in the pore-space. The reduction in hydraulic conductivity only occurs if a) the forced convection physics option is toggled on; and b) a Saturated/Unsaturated Material Model has been applied to regions in which freezing is occurring. The volumetric water content and hydraulic conductivity functions used by the Saturated/Unsaturated material model in the analysis are shown in Figure 4 and Figure 5, respectively. The volumetric water content function was estimated using the sand sample material with a saturated water content of 0.1. The hydraulic conductivity function was estimated using a saturated hydraulic conductivity of 9.77 x 10^{-4} m/sec and a residual water content of 0.005 (Figure 4). The minimum hydraulic conductivity was set to 9.77 x 10^{-10} m/sec (McKenzie et al., 2007).

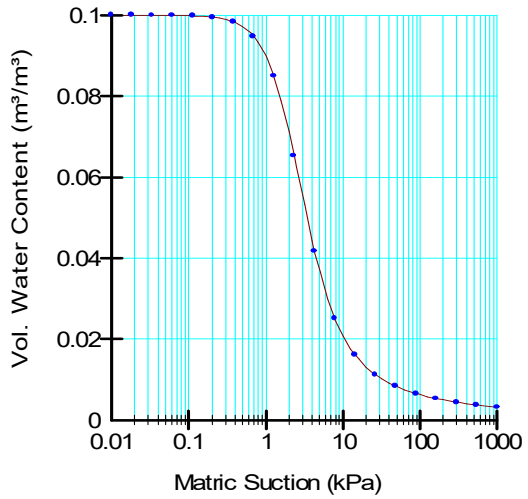

Figure 4. VWC function estimated using the Sand sample type in SEEP/W.

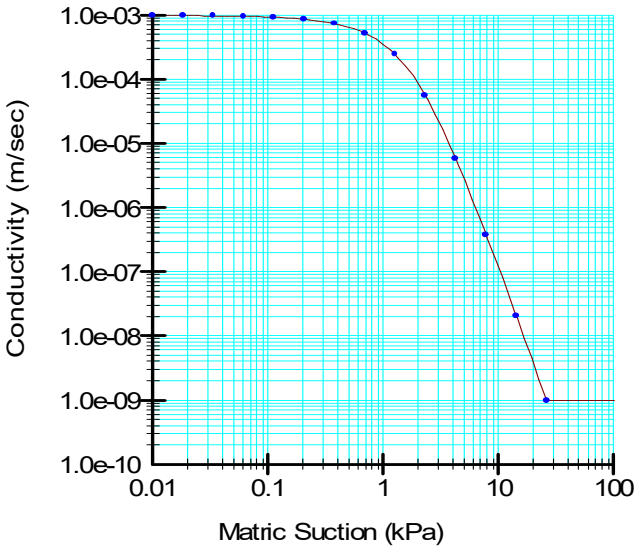

Figure 5. Hydraulic conductivity function.

The conductivity of frozen soil is determined during solution by first calculating the pore-water pressure via the Clausius–Clapeyron equation. The conductivity is determined from the function using the greater of the simulated or calculated negative pore-water pressure. In this example, the soil is completely saturated so the negative pore-water pressure calculated via Clausius–Clapeyron will always be used in frozen parts of the domain to determine the conductivity from the function.

The Simplified Thermal Model was used to characterize the thermal behavior of the soil. The frozen soil thermal conductivity (K_f) can be estimated using the following relationship:

$$K_f = (K_i)^n (K_s)^{1-n} \qquad \text{Equation 1}$$

where K_i and K_s are the ice and soil matrix thermal conductivities and *n* is the soil porosity. The saturated, unfrozen soil thermal conductivity ($K_{unfrozen}$), can be estimated using the following relationship:

$$K_{unfrozen} = (K_w)^n (K_s)^{1-n} \qquad \text{Equation 2}$$

where K_w is the fluid matrix thermal conductivity. The volumetric specific heat capacity (C) can be estimated using the following relationship:

$$C = \gamma_d [c_s + c_w w_u + c_i w_f] \qquad \text{Equation 3}$$

where γ_d is the dry density of the soil, c_s, c_w and c_i are the specific heat of the soil particles, water and ice, respectively, and w_u and w_f are the unfrozen and frozen water contents.

Figure 6 shows the thermal properties of the soil calculated using the aforementioned relationships and the properties shown in Table 1. The frozen volumetric specific heat capacity was calculated assuming an unfrozen water content equal to the residual water content (0.005), making the frozen water content equal to the remaining pore space (n – 0.005). Conversely, the unfrozen volumetric specific heat was calculated using an unfrozen water content equal to the porosity and a frozen water content of zero.

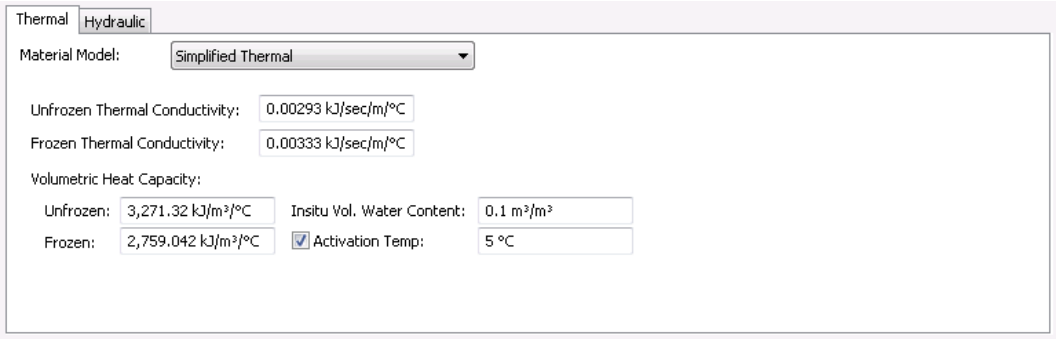

Figure 6. Thermal material properties used in the Simplified thermal model.

The simulation was solved for a total of 800 days using an exponential time stepping sequence with an initial time step of 2 hours.

Results and Discussion

The resulting temperature profiles along the bottom of the domain after a simulation time of 50, 150, 400 and 800 days are shown in Figure 7. The freezing temperatures are conducted both upstream and downstream, until the upstream conduction reaches a maximum extent given the water flow occurring across the domain. The freezing temperatures continue to decrease the temperature of the domain downstream, as the frozen wall removes the heat and energy from the groundwater via conduction.

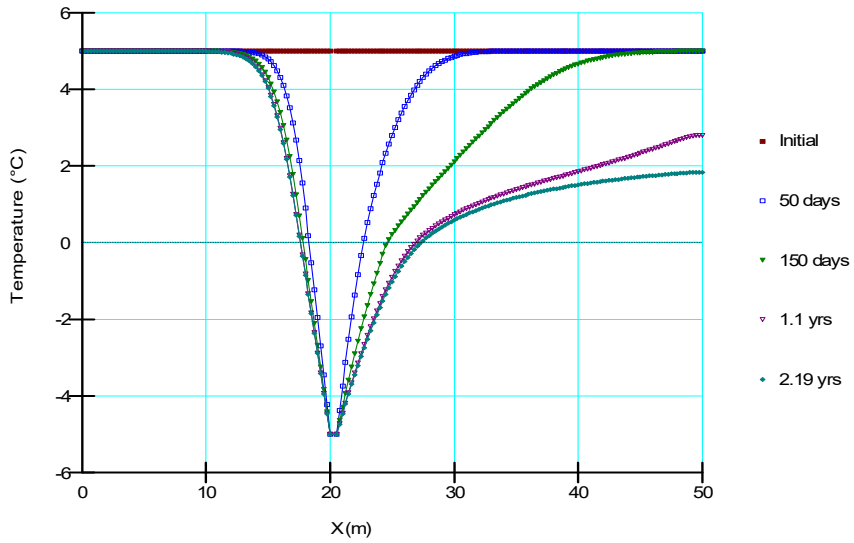

Figure 7. Temperature changes along the bottom of the domain.

As the frozen zone propagates outwards from the original wall, water is forced to flow through the unfrozen soil where the conductivity has not been reduced by pore-ice blockage. Fixing the head on either side of the domain results in an overall decrease in water volume crossing the domain. Regardless, the flux of water above the wall increases relative to other parts of the domain, as is evidenced by the flow vectors, because the area for flow above the wall has decreased (Figure 8). To graph this increase in water rate above the frozen wall, a subdomain can be used in the graphing options. In this example, the subdomain has been set on the elements above the frozen wall and a node location along the upstream edge of the subdomain was chosen (Figure 9). This allows the user to graph the rate of water moving into the elements of the subdomain (Figure 10). As evident in the figure, the water rate increases as the pore ice blockage decreases the flow path area.

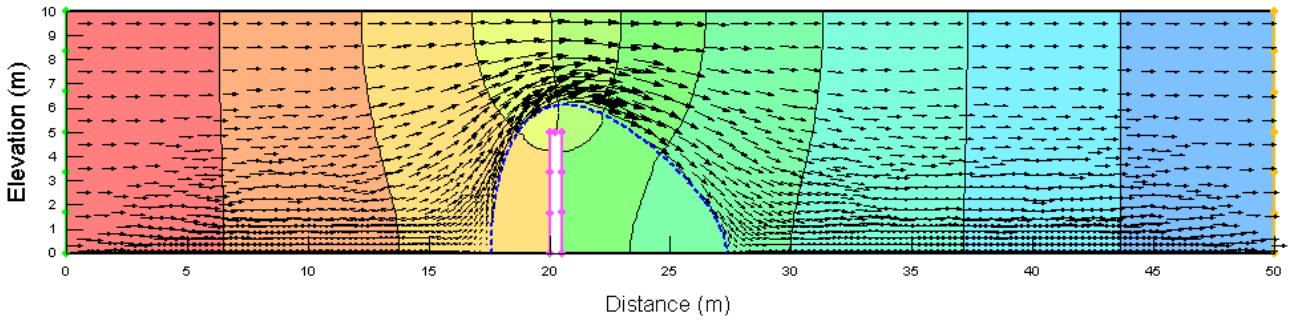

Figure 8. Total head contours with velocity vectors.

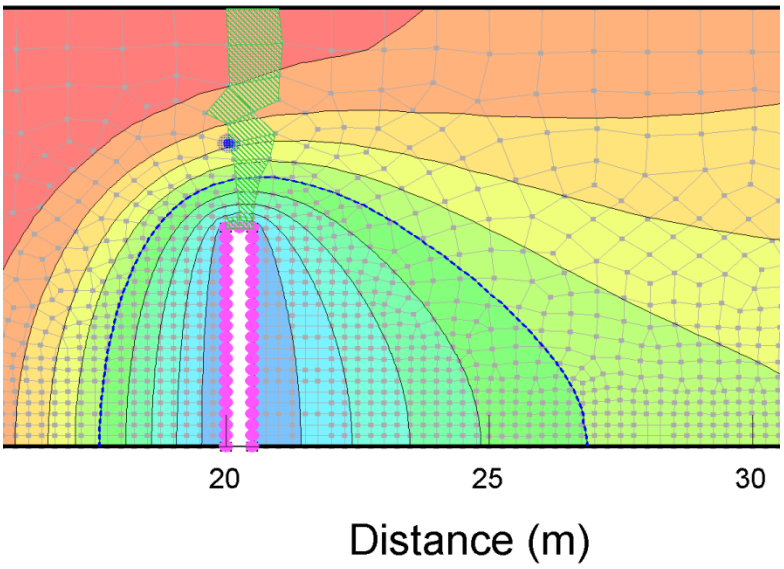

Figure 9. Setting the subdomain and location for water rate.

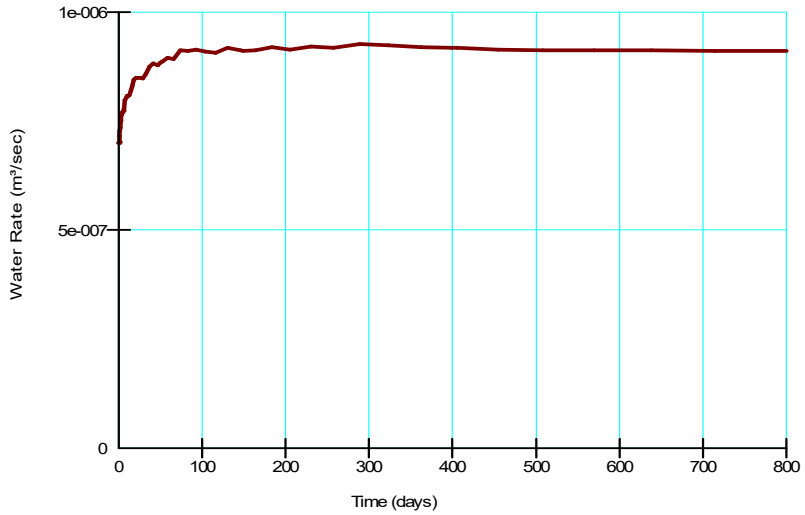

Figure 10. Water flux versus time at node above frozen zone.

Figure 11 shows the extent of the pore blockage in the domain, where an unfrozen water content of 0 indicates soil pores that are completely filled with ice. The Simplified thermal model assumes that water freezes instantly when the temperature drops below the phase change value. As a result, the contours of unfrozen water content are very tightly spaced in a thin 'ring' around the zero temperature contour. McKenzie et al. (2007) simulated a similar response because the authors used a steep unfrozen water content curve (Figure 11).

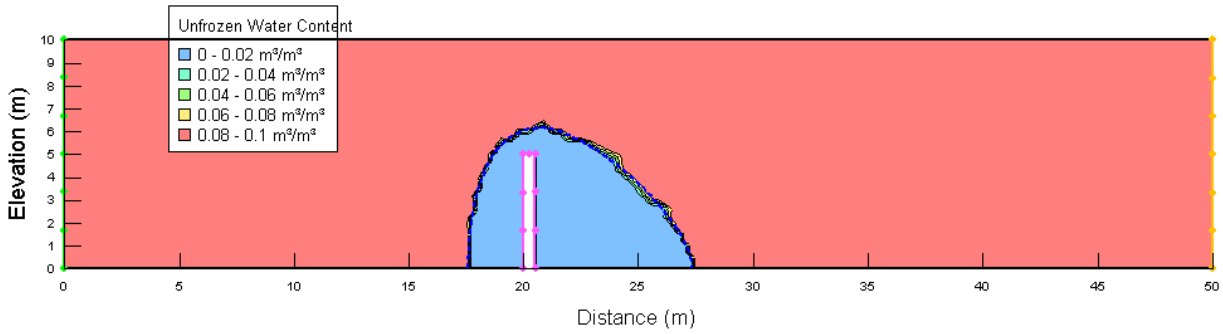

Figure 11. Unfrozen water content contours on day 800.

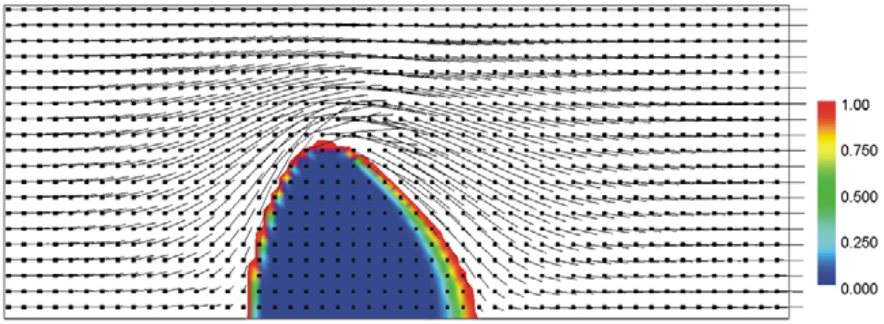

Figure 12. Unfrozen water saturation contours given by McKenzie et al. (2007) for day 800 using the Exponential Freezing Function.

Figure 13 and Figure 14 are the temperature contours at Day 400 simulated by GeoStudio and McKenzie et al. (2007). GeoStudio simulated an upstream and downstream propagation of the zero Celsius contour of about 2.5 m and 7 m, respectively. McKenzie et al. (2007) simulated a much larger propagation of the zero Celsius contour of 5.8 and 18.8 m, respectively. The extent of the zone of frozen water simulated by GeoStudio matches that shown by McKenzie et al. (2007) despite the difference in the temperature contours (compare Figure 11 with Figure 12). McKenzie et al. (2007) used an exponential freezing function, which explains why the frozen zone shown in Figure 12 does not completely envelope the soil within the zero contour (Figure 14). The discrepancy in the temperature contours, however, is likely the result of the inclusion of thermal dispersivity in the SUTRA-ICE formulation used by McKenzie et al. (2007). Thermal diffusivity enhances heat conduction in areas of high water flux, such as above the wall. The increased heat conduction in-turn causes more heat energy to be removed from the domain, allowing the cooler temperatures to propagate further downstream.

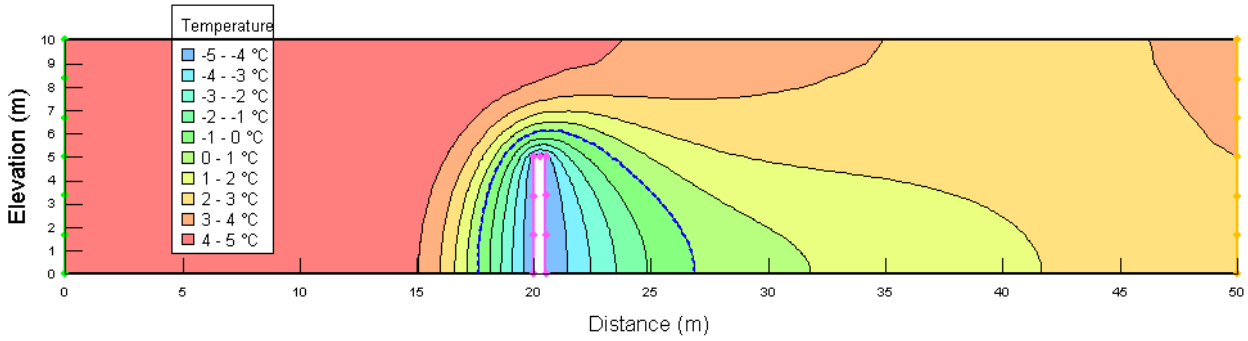

Figure 13. Temperature contours from the TEMP/W analysis on day 400.

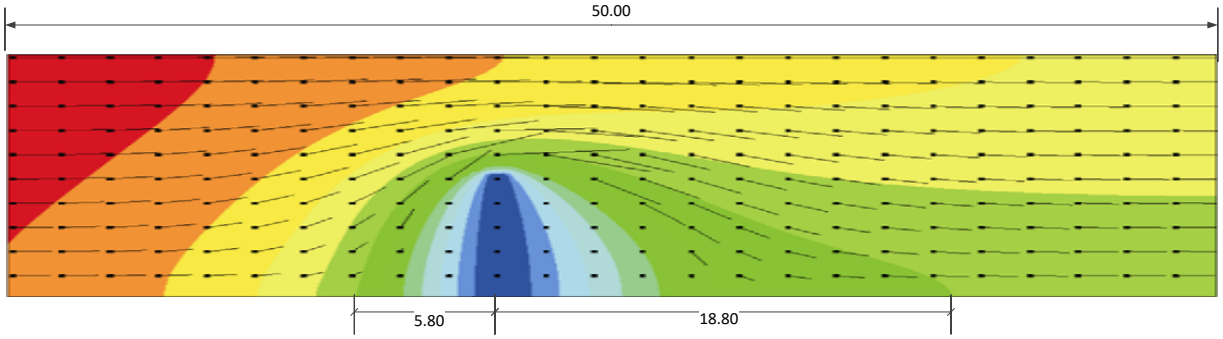

Figure 14. Results for the EXP method at 400 days in McKenzie et al. (2007).

Summary and Conclusions

A simplified TEMP/W analysis was used to explore the effect of a penetrating frozen wall on the thermal regime and groundwater flow of a small areal section. This example was based on an example proposed by McKenzie et al. (2007). The numerical analysis revealed the significant role of ground freezing on groundwater velocity, flow and thermal patterns. As ice formation increased and hydraulic conductivity near the frozen wall decreased, water velocities through the decreasing unfrozen area increased. Temperatures upstream neared steady state more quickly given the constraints imposed by flowing warm groundwater, while downstream the temperature patterns were influenced by the frozen wall more significantly.

References

McKenzie, J.M., Voss, C.I. and Siegel, D.I. 2007. Groundwater flow with energy transport and water-ice phase change: numerical simulations, benchmarks, and application to freezing in peat bogs. Advances in Water Resources, 30, 966-983. Elsevier Ltd.